ChemComm

COMMUNICATION

View Article Online
View Journal | View Issue

Cite this: *Chem. Commun.*, 2014, **50**, 3367

Received 8th December 2013,
Accepted 7th February 2014

DOI: 10.1039/c3cc49319a

www.rsc.org/chemcomm

Dual-responses for electrochemical and electrochemiluminescent detection based on a bifunctional probe†

Jing Han, Ying Zhuo,* Yaqin Chai and Ruo Yuan*

A bifunctional probe (PTC-Tb) which acts as not only a well-defined and stable electrochemical redox molecule but also as a highly efficient co-reactant of an electrochemiluminescent oxygen–peroxydisulfate system was firstly synthesized and applied to the construction of dual-response aptasensors for thrombin detection.

Aptamer, an artificial oligonucleic acid, can bind with high affinity and specificity to a wide range of targets,[1] such as proteins,[2] small molecules,[3] cells,[4] viruses,[5] *etc.* Recently, various aptamer-based biosensors have been developed based on different analytical techniques, such as fluorescence,[6] colorimetric analysis,[7] ultraviolet absorbance,[8] electrochemical (EC)[9] and electrochemiluminescent (ECL)[10] methods. Among them, the EC technique owing to its distinct advantages of simplicity, fast response as well as relatively cheap cost, and the ECL technique owing to its intrinsic advantages of high sensitivity, excellent selectivity as well as low background have been widely used in aptasensors.[11,12] More inspiringly, the dual EC and ECL detection strategy can provide an easier and more effective way as well as a wider dynamic concentration response range for the analysis of targets than the single EC or ECL detection alone. The development of dual-response mode could lead to more rapid clinical decision making and corresponding reduction in patient stress and healthcare costs.[13]

Nevertheless, it is hard to achieve dual-responses for EC and ECL detection on the basis of one aptasensor. Usually, the EC or the ECL aptasensor is indispensable to label its signal probe, so it is difficult to search for a bifunctional probe with the dual EC and ECL responses. Up to now, dual-response modes have been mainly developed based on the heterogeneous biosensors. For example, Zhang's group[14] constructed two distinct biosensors utilizing various probes (magnetic bead-Au-CdS and magnetic bead-Ru biocomplex) to achieve dual-responses for the determination of Ramos cells. Next, Jie and colleagues[15] also designed two different biosensors but one bi-functional probe (quantum dot nanocluster) on the different sensing platform to obtain dual-responses for analysis of the targets (DNA and cancer cells). Furthermore, owing to the dual EC and ECL-properties of $Ru(bpy)_3^{2+}$ itself, Dennany and coworkers[16] developed a sensor using $[Ru(bpy)_2(PVP)_{10}]^{2+}$ assembled layer-by-layer with DNA as a sensing platform to achieve EC and ECL detection. However, because of the inherent water-solubility of $Ru(bpy)_3^{2+}$ and its derivatives, it is difficult to overcome the leakage of the Ru complex from the modified electrode, which limited the development of the Ru complex based solid-state ECL biosensors. To date, with the exception of the $Ru(bpy)_3^{2+}$ system, there has been no report focusing on one biosensor for dual-response detection based on other systems. The reason may be that it is difficult to search for a bifunctional probe with dual-responses for EC and ECL signals.

Perylene-3,4,9,10-tetracarboxylic acid (PTCA), an archetypal π-stacking organic perylene dye, has been widely acknowledged as one of the most promising and rapidly emerging research areas for advanced materials owing to its large specific surface area and low manufacturing cost as well as desirable organic electronic and optical properties.[17–20] Interestingly, PTCA could considerably enhance the ECL signal of peroxydisulfate ($S_2O_8^{2-}$) emission, which has been demonstrated in our previous work.[21] With the goal of obtaining a bifunctional EC and ECL probe, toluidine blue (Tb), which is a kind of dye molecule exhibiting reversible redox-activity, was conjugated to PTCA (the product was abbreviated as PTC-Tb). Herein, the dual-response PTC-Tb probe was firstly synthesized and applied to biosensor construction. We find that PTC-Tb exhibits good membrane-forming properties for the electrode surface modification. More importantly, this bifunctional PTC-Tb probe acts as not only a stable redox molecule with a pair of well-defined EC redox peaks but also as a highly efficient co-reactant of the O_2–$S_2O_8^{2-}$ system for greatly enhancing ECL emission.

In view of the advantageous features of the bifunctional PTC-Tb probe, the dual-response EC and ECL aptasensors were designed to detect thrombin based on one sensing platform which was constructed by a covalently immobilized thrombin

Education Ministry Key Laboratory on Luminescence and Real-Time Analysis, College of Chemistry and Chemical Engineering, Southwest University, Chongqing 400715, PR China. E-mail: yingzhuo@swu.edu.cn, yuanruo@swu.edu.cn; Fax: +86-23-68253172; Tel: +86-23-68252277

† Electronic supplementary information (ESI) available. See DOI: 10.1039/c3cc49319a

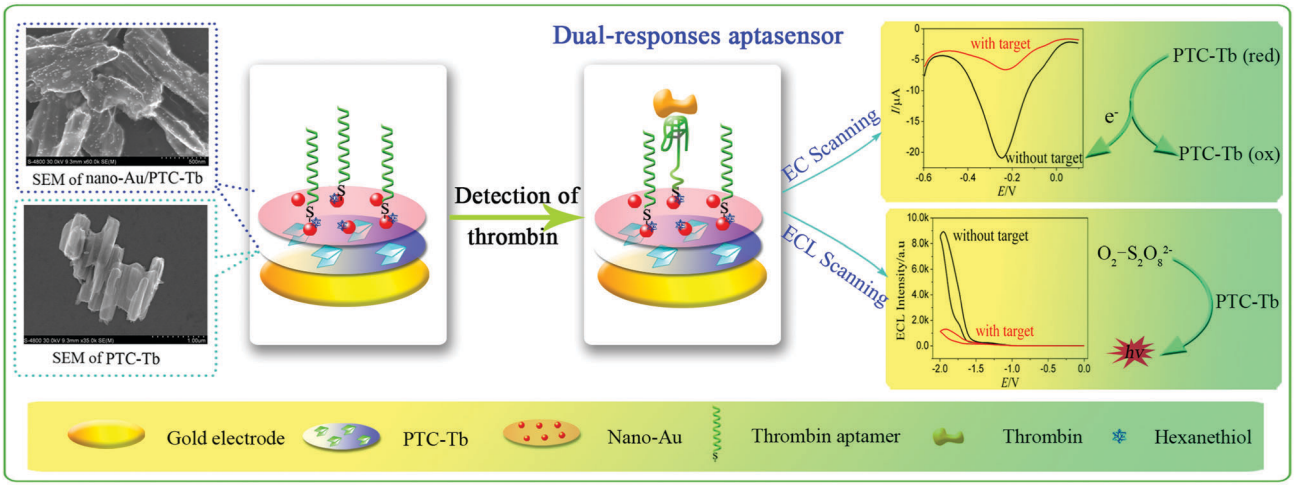

Scheme 1 Schematic illustration of the aptasensor preparation process and dual-responses for EC and ECL detection.

aptamer on the hexanethiol/nano-Au/PTC-Tb modified gold electrode. After incubation with the target, the dual-response EC and ECL signals were obtained and decreased with increasing concentrations of thrombin.

Scheme 1 shows the schematic diagram for the fabrication of aptasensors and dual-response detection of thrombin. First, 5 μL PTC-Tb was coated on a pretreated gold electrode (AuE) and dried in air. Then the PTC-Tb modified electrode was immersed into 2 mL colloidal nano-Au for 4 h to obtain the nano-Au/PTC-Tb modified electrode *via* electrostatic interaction. Subsequently, the prepared nano-Au/PTC-Tb/AuE was incubated with 15 μL of 2 μM TBA for 16 h at room temperature. Following this, the resulting electrode was blocked with 15 μL of 1.0 mM hexanethiol (HT) for 45 min to avoid the nonspecific adsorption. After every step, the modified electrode was extensively rinsed with doubly distilled water to remove nonspecific adsorption and dried under a stream of nitrogen prior to EC and ECL characterization. The obtained aptasensor was stored at 4 °C when not in use.

The fabrication process for the dual-response aptasensor was monitored by EC and ECL characterization. As shown in Fig. 1A, CVs of different modified electrodes for EC characterization were recorded for HAc-NaAc (pH 5.5) at a scan rate of 50 mV s^{-1}. No obvious redox peaks are observed at bare AuE (Fig. 1A, curve a). Nevertheless, when PTC-Tb was modified onto the AuE, a pair of well-defined peaks could be obtained (Fig. 1A, curve b), which were attributed to the excellent electrochemical activity of PTC-Tb. After adsorbing nano-Au on the PTC-Tb membrane, the redox peak current is further improved (Fig. 1A, curve c), which indicates that the nano-Au is similar to a conducting wire, making the electron transfer easier. The peak current decreased obviously, however, when TBA was assembled on the electrode surface (Fig. 1A, curve d). The reason for this is that the aptamer assembled on the electrode can block the electron transfer of the redox probe. Subsequently, non-electroactive HT was employed to block nonspecific sites on the electrode surface and the peak current decreased further (Fig. 1A, curve e). Finally, after incubation with thrombin, the CV response is decreased again owing to the fact that the complementary pairing of thrombin and TBA retards the electron transfer tunnel (Fig. 1A, curve f).

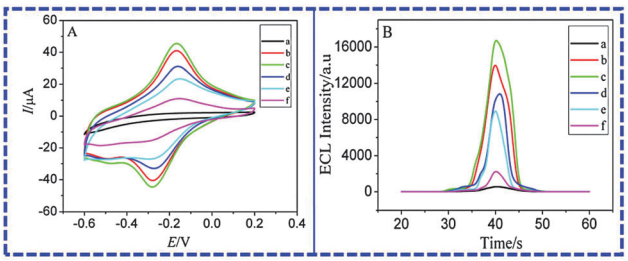

Fig. 1 (A) CV responses of different electrodes in 0.1 M HAc-NaAc buffer (pH 5.5) at a scan rate of 50 mV s^{-1} and (B) ECL responses of different electrodes in 0.1 M HAc-NaAc buffer (pH 5.5) containing 5 mM $K_2S_2O_8$ (the voltage of the photomultiplier tube was set at 800 V) at a scan rate of 100 mV s^{-1}: (a) bare AuE; (b) PTC-Tb/AuE; (c) nano-Au/PTC-Tb/AuE; (d) TBA/nano-Au/PTC-Tb/AuE; (e) HT/TBA/nano-Au/PTC-Tb/AuE; (f) after incubation with 5 nM thrombin.

Furthermore, in order to characterize the fabrication process of the ECL aptasensor, ECL signals at each immobilization step were also recorded. In Fig. 1B, the bare AuE in the O_2–$S_2O_8^{2-}$ system produced a weak ECL response (Fig. 1B, curve a). Upon modifying PTC-Tb on AuE, a remarkable ECL increase is observed (Fig. 1B, curve b), demonstrating that PTC-Tb is a highly efficient co-reactant of the ECL O_2–$S_2O_8^{2-}$ system. The ECL response is increased after adsorbing nano-Au on the PTC-Tb film *via* electrostatic interaction (Fig. 1B, curve c), because nano-Au accelerated the electron transfer in ECL reaction. When TBA was immobilized onto the nano-Au/PTC-Tb/AuE, the ECL signal decreased apparently (Fig. 1B, curve d) for which TBA hinders the diffusion of luminescent reagents toward the electrode surface. The decreased ECL response is also observed after immersing HT to block the nonspecific adsorption on the electrode surface (Fig. 1B, curve e). Finally, the ECL intensity further decreased (Fig. 1B, curve f) after incubation with thrombin, due to forming the complementary pairing blocking layer. As a result, we can make a conclusion that the thrombin has been successfully immobilized on the base electrode.

The performance of the proposed aptasensor was monitored by incubating with 15 μL thrombin standard solutions based on

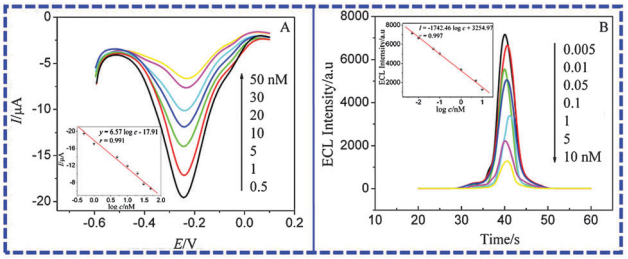

Fig. 2 (A) DPV and (B) ECL responses of the proposed aptasensor after incubation with different concentrations of thrombin (insets: the corresponding calibration curves).

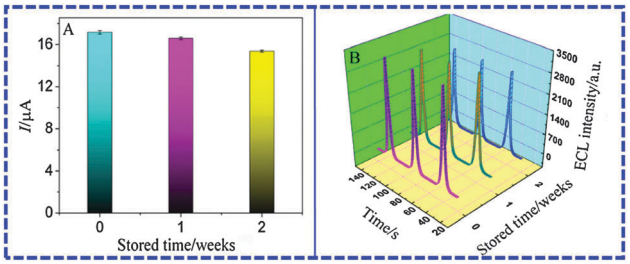

Fig. 3 (A) EC and (B) ECL stabilities of aptasensor for 0 week, 1 week and 2 weeks, respectively (error bars: SD, n = 3).

the developed protocol under the optimal conditions. The DPV current (Fig. 2A) and ECL intensity (Fig. 2B) of the aptasensor decreased with increasing concentration of thrombin. The calibration plot shows a good linear relationship between DPV responses and the logarithmic value of thrombin concentrations ranging from 0.5 nM to 50 nM with a correlation coefficient of 0.991 (Fig. 2A, inset). The regression equation is I (μA) = −6.57 log c (nM) − 17.91 with a detection limit of 0.2 nM (defined as 3σ, in which σ is the relative standard deviation of a blank solution, n = 15). Furthermore, the calibration plot exhibits a good linear relationship between the ECL peak intensities and the logarithmic value of thrombin concentrations ranging from 0.005 nM to 10 nM with a correlation coefficient of 0.997 (Fig. 2B, inset). The regression equation is I (μA) = −1742.46 log c (nM) + 3254.97 (where I is the ECL intensity and c stands for the concentration of thrombin) with a detection limit of 1.7 pM (3σ). With the mutual calibration of EC and ECL curves, a wide dynamic concentration response range of 0.005–50 nM is obtained. This dual-response aptasensor provides an easier and more effective way as well as a wider dynamic concentration response range to accurately detect thrombin.

When the aptasensor was not in use, it was stored at 4 °C to keep the temperature constant. The stability of the proposed aptasensor was measured by a long-term storage assay after incubation with 1 nM thrombin, as shown in Fig. 3. It is found that about 96.7% and 93.8% of the original EC and ECL responses were retained after 1 week, and about 89.7% and 87.2% of the initial EC and ECL signals were noticed after 2 weeks, respectively, indicating that our proposed aptasensor is of acceptable stability.

In summary, a simple dual-response aptasensor has been designed for thrombin detection by employing a bifunctional PTC-Tb probe to construct one sensing platform. Interestingly, the PTC-Tb probe is easily prepared and acts as not only a well-defined and stable EC redox molecule but also as a highly efficient co-reactant of the ECL O_2–$S_2O_8^{2-}$ system. More importantly, the present assays can provide easier and more effective way as well as a wider dynamic concentration response range for the accurate detection of proteins. We believe that this dual-response biosensor may open a new exciting avenue for target detection.

This research was supported by the NNSF of China (21275119, 21105081, 21075100), the Research Fund for the Doctoral Program of Higher Education (RFDP) (20110182120010), Ministry of Education of China (Project 708073), the Specialized Research Fund for the Doctoral Program of Higher Education (20100182110015) and the Natural Science Foundation Project of Chongqing City (CSTC-2010BB4121, CSTC-2009BA1003), the Fundamental Research Funds for the Central Universities (XDJK2010C062, XDJK2012A004), China.

Notes and references

1 S. P. Song, L. H. Wang, J. Li, J. L. Zhao and C. H. Fan, *TrAC, Trends Anal. Chem.*, 2008, **27**, 108.
2 J. Li, H. E. Fu, L. J. Wu, A. X. Zheng, G. N. Chen and H. H. Yang, *Anal. Chem.*, 2012, **84**, 5309.
3 L. Wu, X. H. Zhang, W. Liu, E. H. Xiong and J. H. Chen, *Anal. Chem.*, 2013, **85**, 8397.
4 H. Y. Liu, S. M. Xu, Z. M. He, A. P. Deng and J. J. Zhu, *Anal. Chem.*, 2013, **85**, 3385.
5 M. Labib, A. S. Zamay, D. Muharemagic, A. V. Chechik, J. C. Bell and M. V. Berezovski, *Anal. Chem.*, 2012, **84**, 1813.
6 L. Zhang, J. P. Lei, L. Liu, C. F. Li and H. X. Ju, *Anal. Chem.*, 2013, **85**, 11077.
7 Y. Huang, J. Chen, S. L. Zhao, M. Shi, Z. F. Chen and H. Liang, *Anal. Chem.*, 2013, **85**, 4423.
8 D. Li, B. Shlyahovsky, J. Elbaz and I. Willner, *J. Am. Chem. Soc.*, 2007, **129**, 5804.
9 J. J. Zhao, C. F. Chen, L. L. Zhang, J. H. Jiang and R. Q. Yu, *Biosens. Bioelectron.*, 2012, **36**, 129.
10 G. M. Nie, Z. M. Bai, W. Y. Yu and J. Chen, *Biomacromolecules*, 2013, **14**, 834.
11 D. W. Zhang, J. Nie, F. T. Zhang, L. Xu, Y. L. Zhou and X. X. Zhang, *Anal. Chem.*, 2013, **85**, 9378.
12 C. Y. Tian, J. J. Xu and H. Y. Chen, *Chem. Commun.*, 2012, **48**, 8234.
13 B. V. Chikkaveeraiah, A. A. Bhirde, N. Y. Morgan, H. S. Eden and X. Y. Chen, *ACS Nano*, 2012, **6**, 6546.
14 C. F. Ding, Y. Ge and S. S. Zhang, *Chem.–Eur. J.*, 2010, **16**, 10707.
15 G. F. Jie, J. Zhang, G. X. Jie and L. Wang, *Biosens. Bioelectron.*, 2014, **52**, 69.
16 L. Dennany, R. J. Forster and J. F. Rusling, *J. Am. Chem. Soc.*, 2003, **125**, 5213.
17 M. Eremtchenko, J. A. Schaefer and F. S. Tautz, *Nature*, 2003, **425**, 602.
18 S. R. Forrest, *Chem. Rev.*, 1997, **97**, 1793.
19 J. E. Weaver, M. R. Dasari, A. Datar, S. Talapatra and P. Kohli, *ACS Nano*, 2010, **4**, 6883.
20 B. H. Wu, D. Hu, Y. J. Kuang, Y. M. Yu, X. H. Zhang and J. H. Chen, *Chem. Commun.*, 2011, **47**, 5253.
21 X. X. Gan, R. Yuan, Y. Q. Chai, Y. L. Yuan, Y. L. Cao, Y. H. Liao and H. J. Liu, *Anal. Chim. Acta*, 2012, **726**, 67.